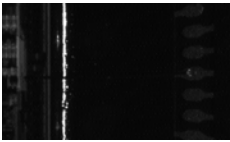
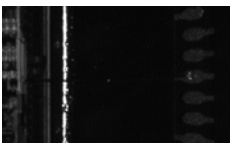
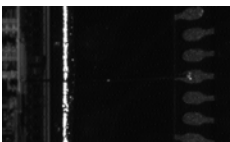
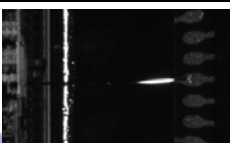
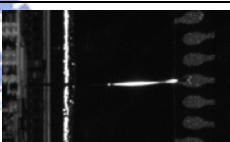
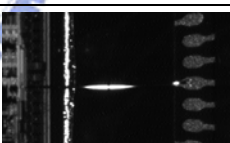
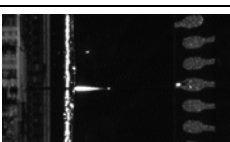
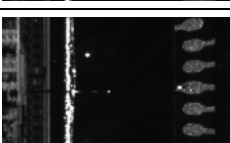
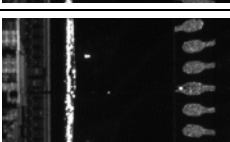
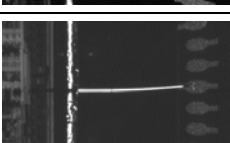


Figure 20. Profile of the tested good bonding wire with the slope of 20 degree

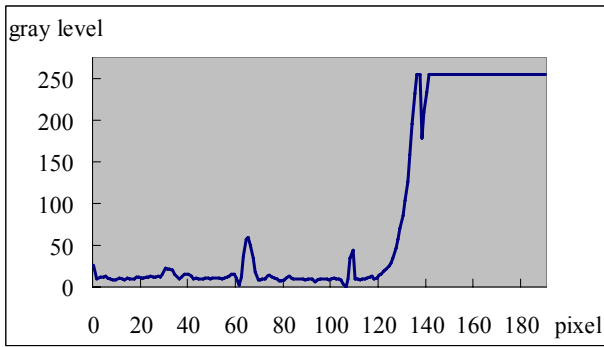


Table 3. The images of a single bonding wire grabbed by turning on some of the LEDs of the developed structured LED lighting system

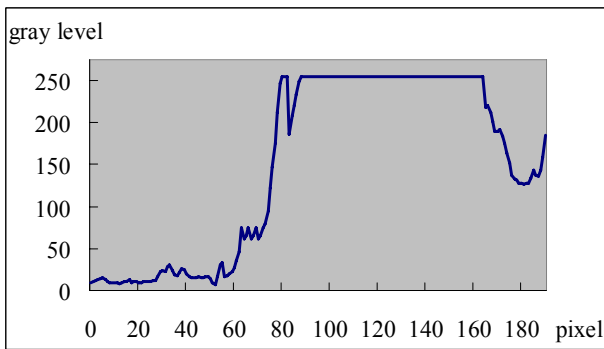
Turned on LEDs	Inclined slope of illuminated wire	Grabbed image
13th	$26\frac{3}{8} \sim 27\frac{5}{8}$ degree	
14th	$25\frac{1}{8} \sim 26\frac{3}{8}$ degree	
15th	$23\frac{7}{8} \sim 25\frac{1}{8}$ degree	
16th	$22\frac{5}{8} \sim 23\frac{7}{8}$ degree	
17th	$21\frac{3}{8} \sim 22\frac{5}{8}$ degree	
18th	$20\frac{1}{8} \sim 21\frac{3}{8}$ degree	
19th	$18\frac{7}{8} \sim 20\frac{1}{8}$ degree	
20th	$17\frac{5}{8} \sim 18\frac{7}{8}$ degree	
21st	$16\frac{3}{8} \sim 17\frac{5}{8}$ degree	
From 16th to 19th	$18\frac{7}{8} \sim 23\frac{7}{8}$ degree	

In Figures 21 (a) to 21(d), we show the gray-level of the pixels on the bonding wires of the grabbed image when the LEDs from the 16th to the 19th rows were turned on individually. The gray-level of the pixels on each of the above wire segments will reach to the maximum value, say 255, if that wire segment is in the slope range that is just proper to reflect the light from the LEDs. Theoretically, each row of the structured LED is designed to highlight a specific slope range of bonding wire. But the light of the LEDs will scatter and the surface of bonding wire will also cause some scattering. That is, the reflective slope range of bonding wire in each row of the structured LED will be larger than the theoretical value. But the enlargement is much smaller than the range of incident light angle of one LED.

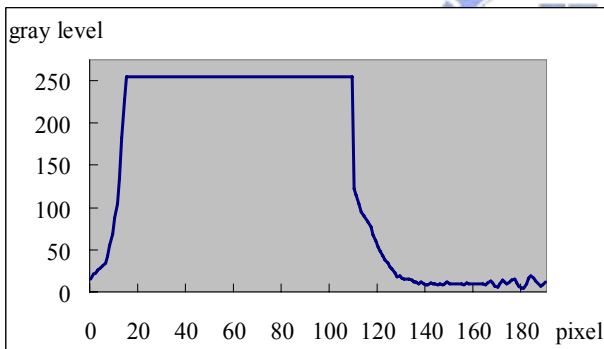
In the developed prototype of structured LED lighting system, if we turn on the LEDs from the 16th to the 19th rows, they will also spread the light to highlight some near by wire segments that will originally be highlighted by the 15th or the 20th row of LEDs. To those bonding wires that are to be highlighted by the LEDs lower than the 14th row or higher than the 21st row will have their pixels with the gray level far lower than 255.



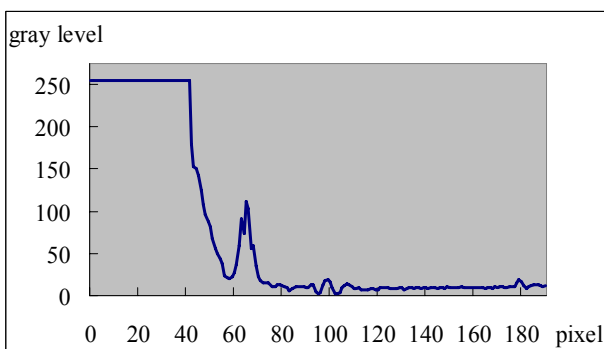
(a)



(b)



(c)

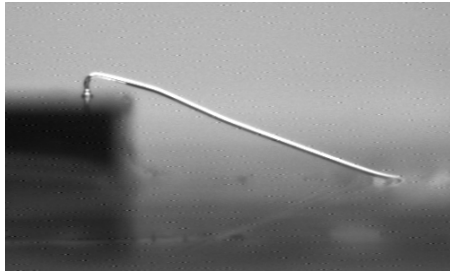


(d)

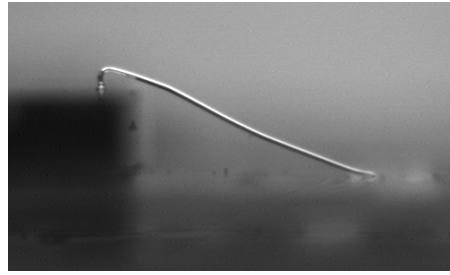
Figure 21. The gray-level of the pixels on the bonding wires of the grabbed images in Table 3 when (a) 16th, (b) 17th, (c) 18th and (d) 19th row of LEDs was turned on.

For 3D-type defect inspection, the developed LED lighting system must provide light with any desired spread range of incident angle to distinguish sagged wires from good wires. The critical segment of good bonding wire sample in this experiment was in about 20 degree slope. A serious drop was found in the critical segment of one sample wire with a slope of 28 degree, while a slight drop was found in the critical segment of the other wire with a slope of 24 degree, as shown in Figure 22. Table 4 shows the grabbed images of a good wire and two sample sagged wires under different spread ranges of incident light angle. The LEDs on the 19th row were set as the center of incident light angle and the spread range of incident light angle increased gradually. The slope ranges of the illuminated wire according to Eq. 4-1 are represented in the first column of Table 4. For the good wire, when the LEDs on the 16th to 22nd rows were turned on, the whole critical segment was illuminated clearly. With the same setting, both the slightly and the seriously sagged wires were represented as a broken line in the grabbed image. That is, both the slightly and the seriously sagged wires can be detected using this setting.

When the LEDs on the 15th to 23rd rows were turned on, the slightly sagged wire was represented as a continuous line, but seriously sagged wire still looked like a broken line in the grabbed image. That is, only seriously sagged wires can be detected using this setting. From these experiments, we can see that the devised structured LED lighting system can distinguish sagged defects in different degree by controlling the spread range of incident light angle. This makes it easy for the AOI system to detect 3D-type sagged defects with various inspection specifications.



(a)



(b)

Figure 22. Profiles of (a) the slightly sagged wires with a drop of 24 degree in slope and (b) the seriously sagged wires with a drop of 28 degree in slope

Table 4. The images of a single bonding wire grabbed for 3D wire inspection by turning on some of the LEDs of the devised structured LED lighting system.

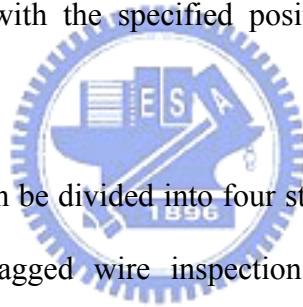
The row of LEDs that were turned on (inclined slope of illuminated wire)	Good wire with the slope of 20 degree	Slightly sagged wire with a drop of 24 degree in slope	Seriously sagged wire with a drop of 28 degree in slope
Only the 19th ( $18\frac{7}{8} \sim 20\frac{1}{8}$ degree)			
From the 18th to the 20th ( $17\frac{5}{8} \sim 21\frac{3}{8}$ degree)			
From the 17th to the 21st ( $16\frac{3}{8} \sim 22\frac{5}{8}$ degree)			
From the 16th to the 22nd ( $15\frac{1}{8} \sim 23\frac{7}{8}$ degree)			
From the 15th to the 23rd ( $13\frac{7}{8} \sim 25\frac{1}{8}$ degree)			
From the 14th to the 24th ( $12\frac{5}{8} \sim 26\frac{3}{8}$ degree)			
From the 13th to the 25th ( $11\frac{3}{8} \sim 27\frac{5}{8}$ degree)			
From the 12th to the 26th ( $10\frac{1}{8} \sim 28\frac{7}{8}$ degree)			

For bonding wire inspection, the light should be set in the proper range of incident angle to illuminate the good wire segment and to have the sagged wire segment be highlighted. That is, we should calculate the slope of the wire in the critical segment and the corresponding row(s) of structured LED lighting system. And then the range of incident light angle (the number of rows of the LED to be turned on ) should be relaxed until all the “good” wire segments are illuminated, according to the specification of wire bonding and Eq. 4-1. After the adjustment, all sagged wire segments can easily be distinguished from the good wire by the AOI system.



## 5. Inspection Algorithms

After grabbing clear images of bonding balls and wires by using proper lighting device, we developed a set of inspection algorithms for further process. In the wire bonding process, the bonding machine will first find the pre-designed calibration marks on the IC chip and the substrate. These marks are designed as the calibrating points to aid locating the substrate and the IC chip. The corresponding data file was read in from a stored file prior to starting the wire bonding process. The CAD data file records the position of the calibrating points and the relative position of each of the pads, leads, and bonding wires. After the calibrating process, the bonding machine will then start the process of connecting each pad to corresponding lead. After the bonding process, the bonding balls and wires in the grabbed images should be compared with the specified positions in the data file to ensure the correctness.



The inspection process can be divided into four steps: bonding ball inspection, shorted wire inspection, lost/broken/sagged wire inspection and shifted wire inspection. The inspection sequence is arranged according to the seriousness of defect type to save inspection time. Besides, the bonding balls and wires have to be inspected under different types of lighting environment, as described in Sections 3 and 4. The images of bonding balls and wires have to be grabbed respectively by using proper lighting devices to complete inspection process. All the bonding balls and wires on the IC chip thereafter can be grabbed and inspected by using algorithm 1. Figure 23 shows the process to grab and inspect all the bonding balls and wires on the IC chip.

### **Algorithm 1: Wire bonding inspection of the IC chip**

**Input:** a data file of the bonding balls and wires

**Output:** the detected defect of the bonding ball and wire



## **Method**

**For** i = 1 to 4 **do**

Grab a serial of images and connect it into image(i) of the bonding wires of one side of the IC chip by using surrounding type lighting device

*/\*image(1), image(2), image(3) and image(4) respectively corresponds to the bonding balls in the north, east, south and west side of the IC chip\*/*

**End for**

Method **Bonding ball inspection**

*/\*Compare the position of the bonding balls in the images with the input data file\*/*

**For** i = 1 to 4 **do**

Grab a serial of images and connect it into image(i) of the bonding wires of one side of the IC chip by using the structured LED lighting system

**End for**

Method **Shorted bonding wire inspection**

*/\*Detect possible shorted defect of the bonding wires\*/*

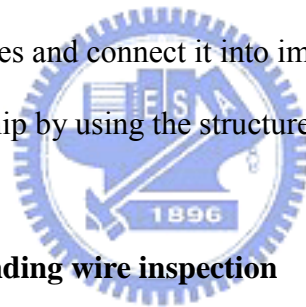
Method **Lost/broken/sagged bonding wire inspection**

*/\*Detect possible broken, lost or sagged defect of the bonding wires\*/*

Method **Shifted bonding wire inspection**

*/\*Detect possible shifted defect of the bonding wires\*/*

**End algorithm 1**



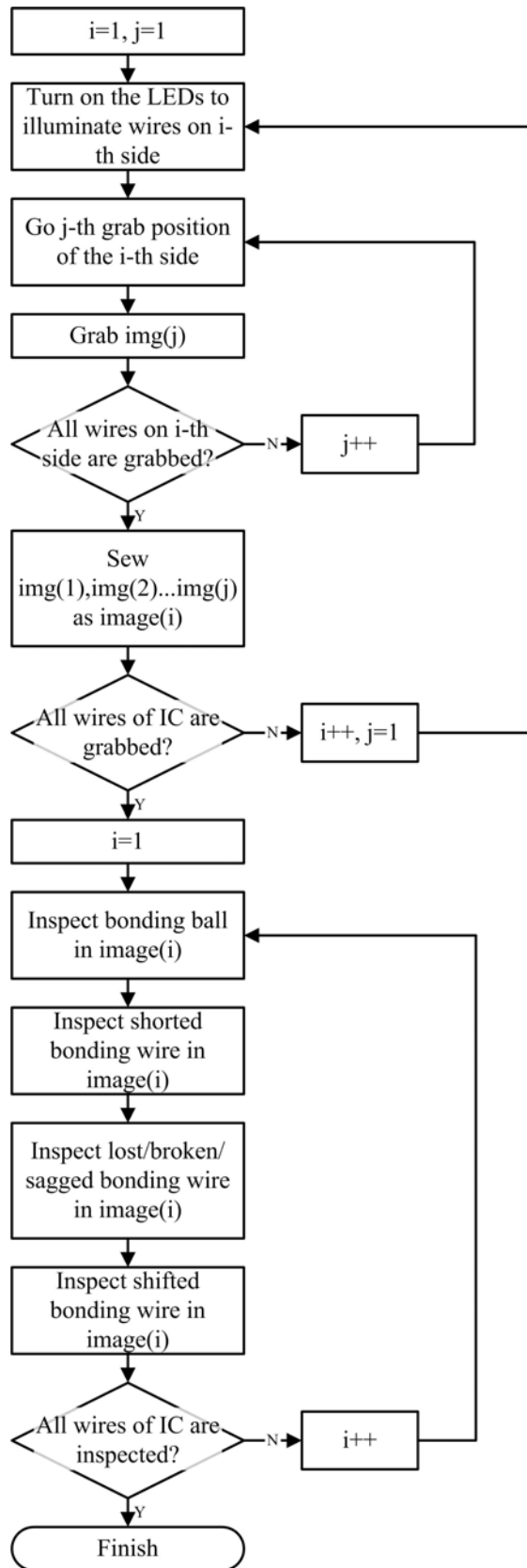


Figure 23. The flowchart of the developed AOI system for image grabbing and bonding wire inspection

## 5-1 Bonding ball inspection

The first inspected item is the position of bonding ball, the starting point of a bonding wire. Former researchers focused on inspecting both the contour shape and the position of the bonding ball. Currently, the bonding machine is good enough that the contour shape of the bonding ball is accepted as it is. Inspectors need only focus on the position accuracy of the bonding ball. The best-fitting ellipse method is usually used to search for the center of bonding ball but it requires a long calculating time. That makes it difficult to synchronize the inspection process with the production line. Therefore, a proper method is required to search for the bonding ball.

Generally, the pattern matching is a popular method to search for objects with similar property in an image. The bonding balls with constant contour should be the suitable objectives but the bonding wires cause a problem. The wire connecting the center of the bonding ball with the lead on the substrate is found in four directions of the image: north, east, south and west. Each connecting direction of the wire with the bonding ball may not be the same, and the shapes of the bonding balls are distinct. Therefore an ordinary pattern matching method cannot be directly applied to search for the bonding ball with variant shapes. In Figures 24, four images of the bonding ball are shown. Each image, as a part of one side image, of the IC chip, has wires connecting with the balls in different direction. We can also see that the bonding balls in one image have similar shapes, but have variant shapes with that of other images.

However, if the lead of a pad was found in the upper portion of the image, then the wire will affect only a small upper part of the contour of the bonding ball. The remaining part (the lower portion) of the ball is still of the same shape. So, we can take the remaining lower portion, which is about 60% of a full bonding ball, as a search model for the modified

pattern matching approach. Similarly, if the bonding wire goes to the lower side, we take the upper 60% part of the full bonding ball as the search model, and similarly for the left and the right side cases. This modified pattern matching method can quickly and accurately search and detect the positions of all the bonding balls in each of the four side images of IC chip.

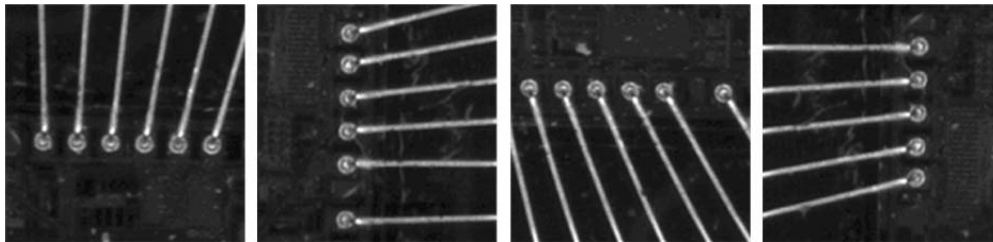


Figure 24. Images of the bonding ball with variant shapes of contour

If the shifted distance of the bonding ball is larger than the allowance, then the connecting bonding wire will be marked as a shifted wire. If a bonding ball is not found in the specified position, the connecting wire will be marked as a lost wire. The bonding wire with defect will be ignored in the next inspection procedure. The method used to check the position of bonding ball is described in Algorithm 2.

#### **Algorithm 2: Bonding ball position inspection**

**Input:** four images of the bonding balls, a data file of the bonding balls, templates of bonding ball

**Output:** the position of each of the bonding balls

**Method** bonding ball inspection

**For**  $i=1$  to 4 **do**

    Calculate the approximate position of the upper-left bonding ball, which is closest to the original point of image( $i$ ), according to the data file of the bonding wire.

Find the first bonding ball in image(i) by modified pattern matching method.

Find out all the other bonding balls in image(i) by modified pattern matching method.

/\* The first bonding ball is used as a reference for later processing\*/

**For** j=1 to B **do**           /\* B is the total number of bonding ball in image(i)\*/

**If** the shifted distance of bonding ball(j) is greater than the allowance

**Then** Mark bonding wire(j) which connecting to bonding ball(j) as a shifted wire.

**Else if** bonding ball(j) is missed

**Then** Mark bonding wire(j) as a lost wire

**End if**

**End for**

**End for**

**End algorithm 2**



## 5-2 Shorted wire inspection

In the bonding wire inspection, the shorted wire will be detected first, followed by the case of lost/broken/sagged wire. The case of shifted wire will be detected lastly.

To inspect a bonding wire, we need to extract the positions of all pairs of the start point (bonding ball) and the end point (lead). First we find the position of each of the bonding balls as described in section 5.1 or directly download the position data from the bonding data file. Then we calculate the position of each of the leads on the substrate. The position of the lead is calculated as follows. A stored image of the calibrating mark is used as a template to detect the positions of a pair of the calibrating marks in the image by the pattern matching method. The relative position of every lead can then be calculated in reference to the input data file of the bonding wires.

As to the errors of the bonding wire itself, the most serious case is shorted defect. The projection method is used to check a rectangular region in which every two adjacent wires are covered. The projection region will only cover the critical segments of the bonding wires which are in a specified range of slope, as illustrated in Figure 25. The number of pixels and accumulative gray-levels in this region are summed together in the direction parallel with the bonding wire. All the bonding wires are marked as the shorted wires first. And then the AOI system will confirm whether every bonding wire connects with the next one or not. If there is no wire connecting the two adjacent wires, the accumulative gray-level will be lower than the background threshold. Then, the inspected bonding wire will be marked as a normal wire. The following Algorithm 3 presents the method for shorted bonding wire inspection.

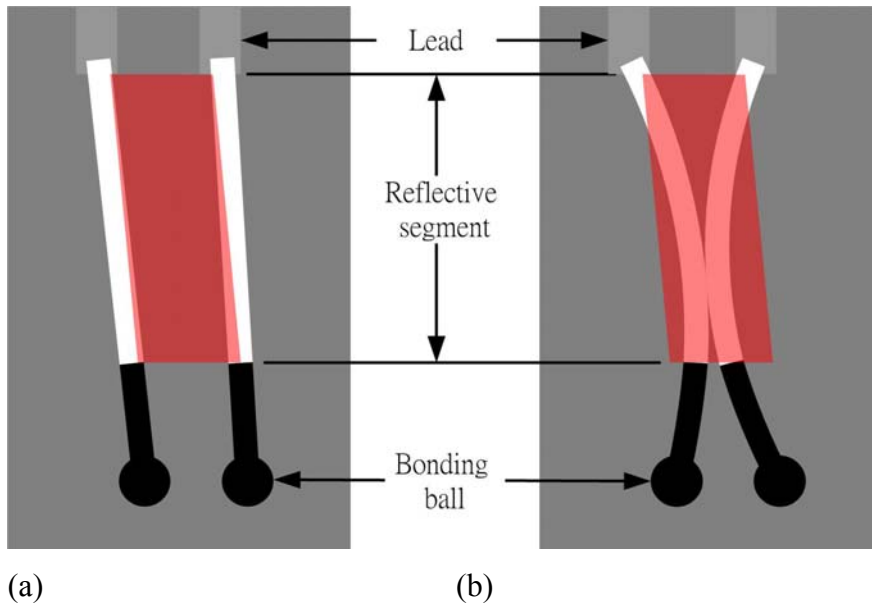


Figure 25. Illustration of the projection regions for (a) a pair of normal wires and (b) a pair of shorted wires. The red rectangular regions indicate the projection regions and the project directions are set as parallel with the wires.

### Algorithm 3: Shorted bonding wire inspection

**Input:** four images of the bonding wires, a data file of the bonding wires

**Output:** the index of shorted wire

#### Method

**For**  $i=1$  to 4 **do**

**For**  $j=1$  to  $W$  **do** /\* $W$  is the total number of bonding wires in image( $i$ )\*/

Calculate the position of the lead of bonding wire( $j$ ), according to the input data file of the bonding wires.

Get the position of pad of the bonding wire( $j$ ) from the bonding ball inspection process or the corresponding data file

Mark wire( $j$ ) as a shorted wire

**End for**

**For**  $j=1$  to  $W-1$  **do**

Get the accumulative gray-levels of projection within the rectangular region

between and parallel with wire(j) and wire(j+1).

**If** one of the accumulative gray-levels is lower than the background value

**Then** Mark wire(j) as a normal wire

**End if**

**End for**

**End for**

**End algorithm 3**

### **5-3 Lost/broken/sagged wire inspection**

By using the LED structured lighting system, the bonding wire in specified range of slope will reflect sufficient light into the camera. In the grabbed image, the gray-level of the pixels that lying on the center of sufficiently reflective wire segment will reach the maximum value (say 255 in an 8-bit grayscale image). If a bonding wire disappears, the gray-level of the pixels lying on the specified position of the wire will be as low as the background value. Due to the incomplete reflection of light, the gray-level of the pixels of the sagged wire segment will be lower than the maximum value but higher than the background value. That is, if we set scan lines which cross the reflective segment of a bonding wire, as illustrated in Figure 26, then the lost, broken or sagged wires can be distinguished from the normal wires by checking the highest gray-levels of the pixels lying on the scan lines. Once a broken wire happened, the tension of the wire will result in a great gap. So, the distance between every two scan lines can be set wider to save calculation time.

The gray-level variance of the pixels between the normal and the sagged wire is caused by the variance of the slope. A sagged wire with minor defect will only reduce the gray-level of its corresponding pixels in the image slightly. But, a serious sagged wire may reduce the gray-level of its corresponding pixel to be as low as the background value. That



is, a serious sagged wire may be inspected as a broken wire. If we want to distinguish serious sagged wire from broken wire, more images grabbed by using different lighting environments are required. The algorithm of lost/broken/sagged bonding wire inspection is described in algorithm 4.

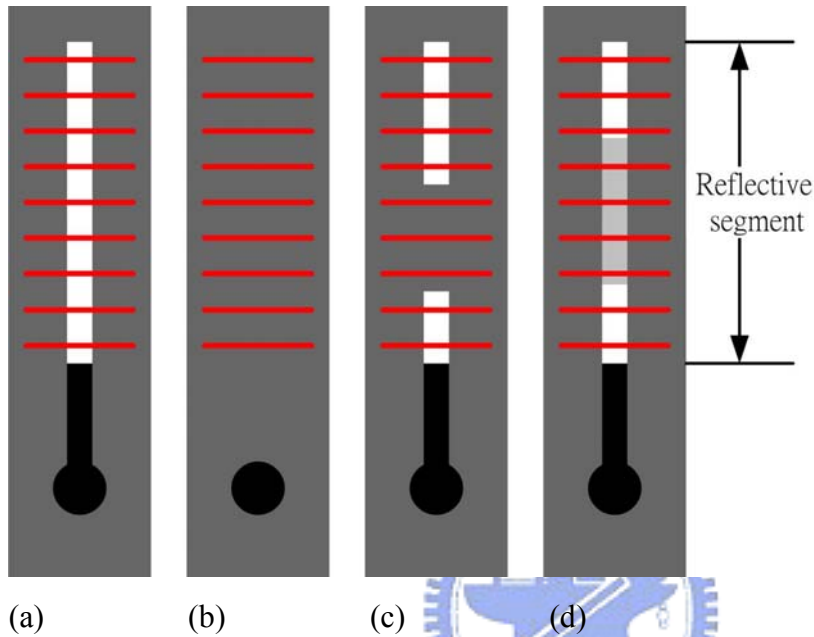


Figure 26. Illustration of the scan lines for lost/broken/sagged wire inspection. The red lines indicate the scan lines of (a) a normal wire (b) a lost wire (c) a broken wire and (d) a sagged wire

**Algorithm 4: Lost/broken/sagged wire inspection**

**Input:** four images of the bonding wires, a data file of the bonding wires

**Output:** the index of lost/broken/sagged wire

**Method**

**For** i =1 to 4 **do**

**For** j = 1 to W **do**           /\* W is the total number of bonding wires in image(i) \*/

        Set scan lines which cross the bonding wire(j) in image(i)

**For** k = 1 to L **do**           /\* L is the total number of scan line\*/

Record the highest gray-level of pixels on scan line(k)

**End for**

**If** each of the highest gray-level of the scan lines of wire(j) is as low as that of background value

**Then** Mark wire(j) as a lost wire

**Else if** some of the highest gray-levels of the scan lines of wire(j) are as low as that of background value

**Then** Mark wire(j) as a broken wire

**Else if** some of the highest gray-level of the scan lines of wire(j) are higher than that of background value but lower than the maximum gray-level

**Then** Mark wire(j) as a sagged wire

**End if**

**End for**

**End for**

**End algorithm 4**



#### **5-4 Shifted wire inspection**

After inspecting the shorted, lost/broken/sagged wires, we continue to detect the last possible case of shifted wire. To save calculation time, only the normal wires in pervious inspection processes are to be inspected. A shifted wire is defined as the bonding wire whose center line shifted away from the pre-defined position by a distance greater than the allowance. Practically, the allowable shifting distance is generally set to be the diameter of the bonding wire. Two scan lines are set in the two boundaries of a bonding wire to check the reflective segment of the bonding wire for shifted wire inspection, as illustrated in Figures 27. The gray-levels of the scan lines have to be checked pixel by pixel. If some part of a bonding wire can not be found in between the two scan lines, then the bonding wire

will be marked as a shifted wire, as illustrated in Figures 27(d) and 27(e).

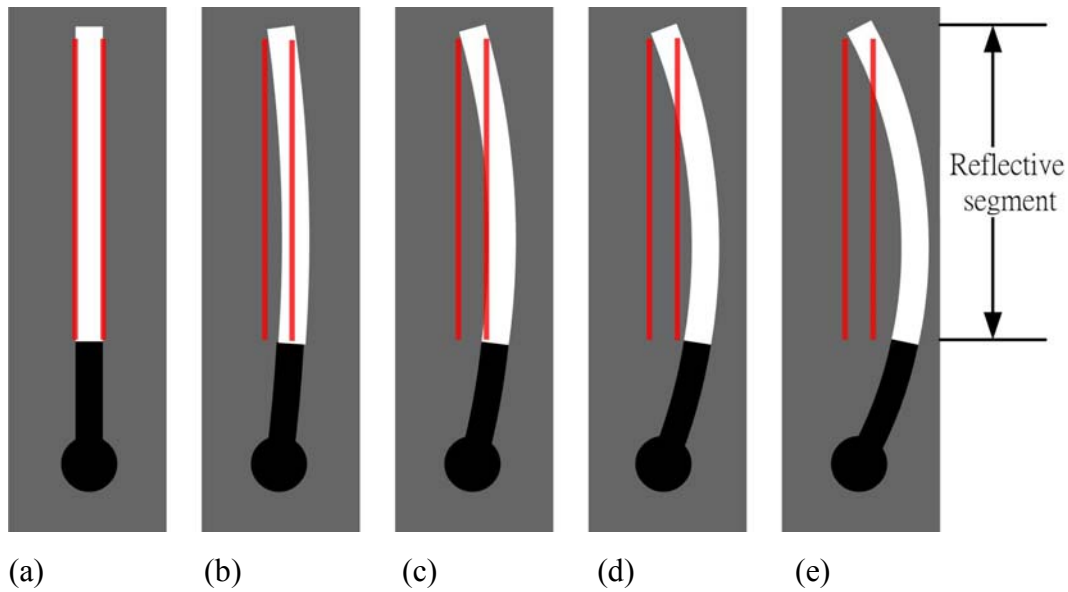


Figure 27. Illustration of scan lines for shifted wire inspection with one diameter specification of (a) a normal wire, (b) a wire shifted away by  $0.5 * \text{diameter}$ , (c) a wire shifted away by  $1 * \text{diameter}$ , (d) a wire shifted away by  $1.5 * \text{diameter}$  and (e) a wire shifted away by  $2 * \text{diameter}$

For larger allowance of the shifted wire, the number of scan lines has to be increased correspondingly. For example, if the allowance is set to be one and half times of the diameter of the bonding wire, then three scan lines are required for the shifted defect inspection, as illustrated in Figures 28. Once a bonding wire shifted by a distance greater than two times of its diameter of the bonding wire, see Figure 28(e), it will be detected as a shifted one. Only when the wire shifted away by a distance greater than the allowance will be marked as a shifted wire, the others will be treated as the normal wires. The algorithm of shifted wire inspection is described in algorithm 5.

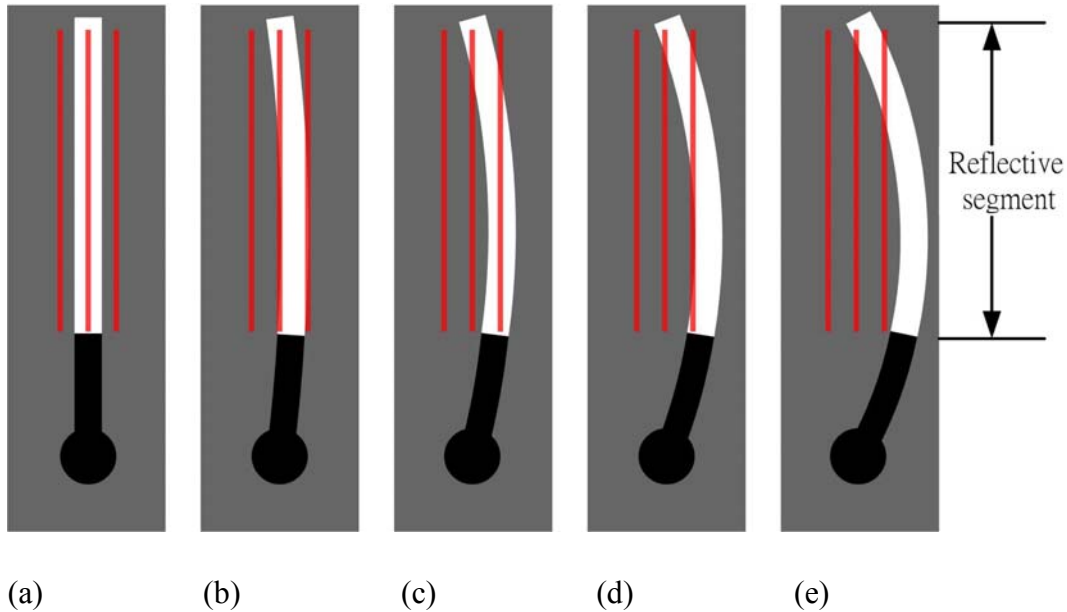


Figure 28. Illustration of scan lines for shifted wire inspection with one and half diameter specification of (a) a normal wire, (b) a wire shifted away by  $0.5 * \text{diameter}$ , (c) a wire shifted away by  $1 * \text{diameter}$ , (d) a wire shifted away by  $1.5 * \text{diameter}$  and (e) a wire shifted away by  $2 * \text{diameter}$

#### Algorithm 5: Shifted wire inspection

**Input:** four images of the bonding wires, a data file of the bonding wires

**Output:** the index of shifted wire

#### Method

**For**  $i=1$  to 4 **do**

**For**  $j = 1$  to  $W$  **do**     /\*  $W$  is the total number of bonding wire in image(i) \*/

**If** wire(j) is not marked as a lost or broken wire

**Then** Set the scan lines along the specified position of wire(j)

                Record the gray-level of pixels of scan lines to verify whether the bonding wire(j) is lying in between the scan lines

**For**  $k=1$  to  $S$      /\*  $S$  is the length of the scan line of wire(j) \*/

**If** the gray-level of the pixel(k) on the scan lines are all lower than that of background value

**Then** Mark wire(j) as a shifted wire  
**Exit for**  
**End if**  
**End for**  
**End if**  
**End for**  
**End for**  
**End algorithm 5**



## 6. Experimentation and Result Analysis

### 6-1 Experimental environment setting

The experimental environment for wire bonding inspection is illustrated in Figure 29. All the images of the bonding balls and bonding wires were grabbed by using a CIS VCC-880A B/W camera of 1600 x 1200 resolution and a Matrox Meteor II grabber. A telecentric lens in 1X optical rate was used and the physical width of one pixel was 4.5 $\mu$ m. The physical size of the inspection window was 7.2mm x 5.4mm. The inspection algorithms were programmed using Microsoft Visual Basic 6.0 and Matrox MIL 7.0. The experimental computer was powered by an Intel Pentium IV 1.7G CPU.

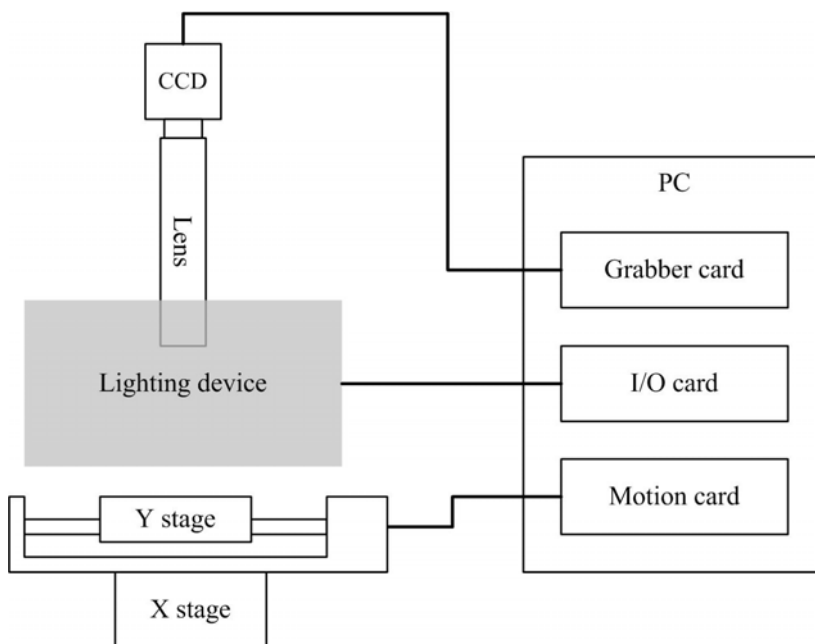


Figure 29. The illustration of experimental equipments for wire bonding inspection

We used an IC chip with 100 bonding wires as the experimental example in this section. The physical size of the experimental IC chip was about 6mm x 6mm and the bonding wires surrounded the chip in the region about 9mm x 9mm. The pitch of the experimental IC, the gap between the two adjacent pads, is about 30  $\mu$ m and almost reaches the minimum value of the commercial product. That is, the resolution of the AOI system is good enough to deal

with the available bonded IC chips. Each image to be inspected will cover 25 bonding wires along one boundary of the IC chip. This inspected image is generated by connecting two images grabbed consecutively. Figure 30 shows a synthesized image of the experimental IC chip.

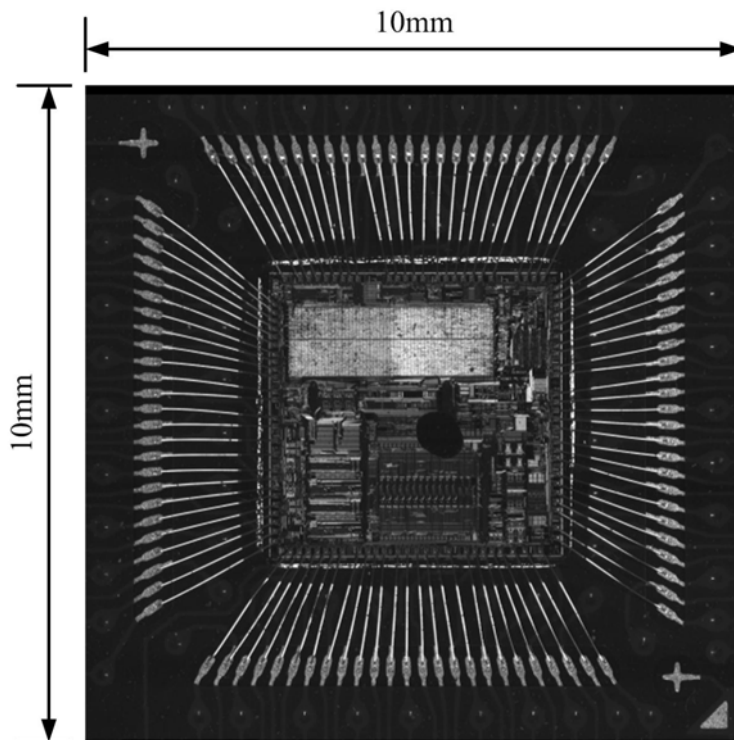


Figure 30. The synthesized image of the experimental IC chip

## 6-2 Experimental result of bonding ball inspection

An exemplified search model, consisting of  $19 \times 14$  pixels, for describing the bonding ball inspection process is shown in Figure 31. According to the position of the calibrating point on the substrate, and the file of the bonding data, we can calculate the approximate region of each of the bonding balls in the image. This search model was used to search for every bonding ball in these regions. Figure 32 illustrates the detected results of the bonding balls of the images corresponding to Figure 24. Each cross-hair in the image represents the determined center of each bonding ball. The correlation coefficient derived by the pattern matching method represents the difference between the search model and the image of the

detected result. All the correlation coefficients of the bonding ball obtained by the proposed approach are higher than 70%. This level of correlation coefficient is qualified for detecting the bonding ball in real practice.



Figure 31. The search model of an exemplified bonding ball (19 x 14 pixels, 4.5um/pixel)

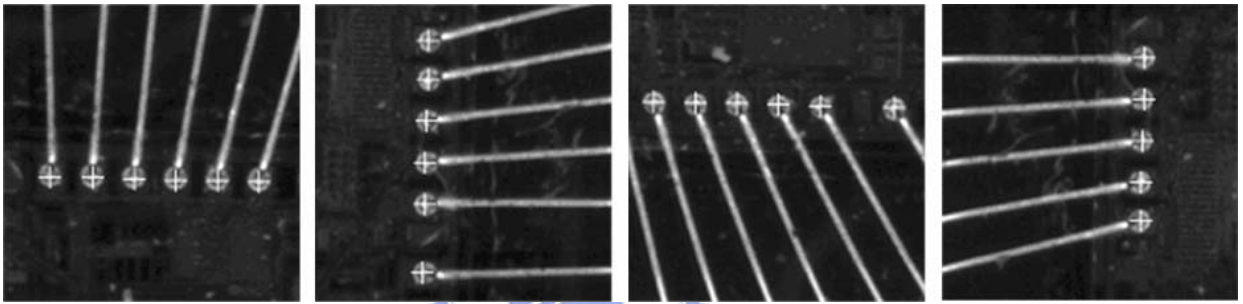


Figure 32. The detected results of bonding balls of the images as shown in Figure 24. The ball with a cross-hair mark means it was found by the proposed pattern matching method.

### 6-3 Experimental result of shorted bonding wire inspection

In inspecting the bonding wire, we need to extract the threshold value of the background of the image first. The bonding wire can then be distinguished from the grabbed image. A region consisting of 100 pixel x 100 pixel without any wire or chip will be selected. And then, the average  $\mu$  and standard deviation  $\sigma$  of the gray-levels of all the 10000 pixels in this region are calculated. Figure 33 illustrate the grabbed and the binarized images with  $\mu+3\sigma$  and  $\mu+6\sigma$  of the gray-level of the background as the threshold. We can see that the image of Figure 33(c) has better thresholding result than Figure 33(b), and hence the value of  $\mu+6\sigma$  of the gray-levels of the background is used as a threshold in later



experimentations.

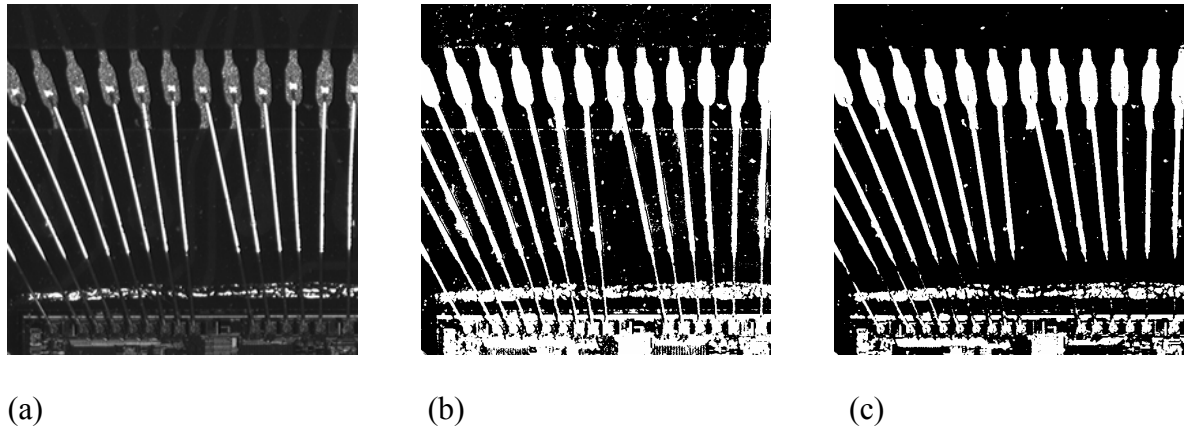


Figure 33. (a) The grabbed image of bonding wires and (b) binarized image with  $\mu+3\sigma$  of the gray-level of background as the threshold and (c) binarized image with  $\mu+6\sigma$  of the gray-level of background as the threshold

After deciding the threshold value, we can inspect the shorted defect of the bonding wires in the image. Figure 34(a) shows an image of bonding wires without shorted defect while Figure 34(b) shows an image with a man-made shorted defect between the 12-th and the 13-th bonding wires. The meshed rectangular regions in the two images indicate the projection regions which were formed by projecting in parallel with the wires. Once a bonding wire was found lying on the projection region, the accumulative gray-level will be higher than the threshold value (say  $\mu+6\sigma$  of the gray-level of background \* height of projection region). That is, if one of the accumulative gray-level of the projection region is lower than the threshold value of the background, then the first wire of the two adjacent wires will be marked as a normal wire. The projection results of the two inspected wires of Figure 34(a) and 34(b) are shown in Figures 34(c) and 34(d), respectively. The squares indicate the accumulative gray-level of projection and the horizontal lines indicate the threshold value of the background. Figure 34(c) shows that many accumulative gray-level values are lower than the background threshold while Figure 34(d) shows all accumulative

gray-level values are greater than the background threshold. That is, the 12-th and 13-th wires in Figure 34(a) are normal wires without shorted defect; while the 12-th and 13-th wires in Figure 34(b) are shorted wires.

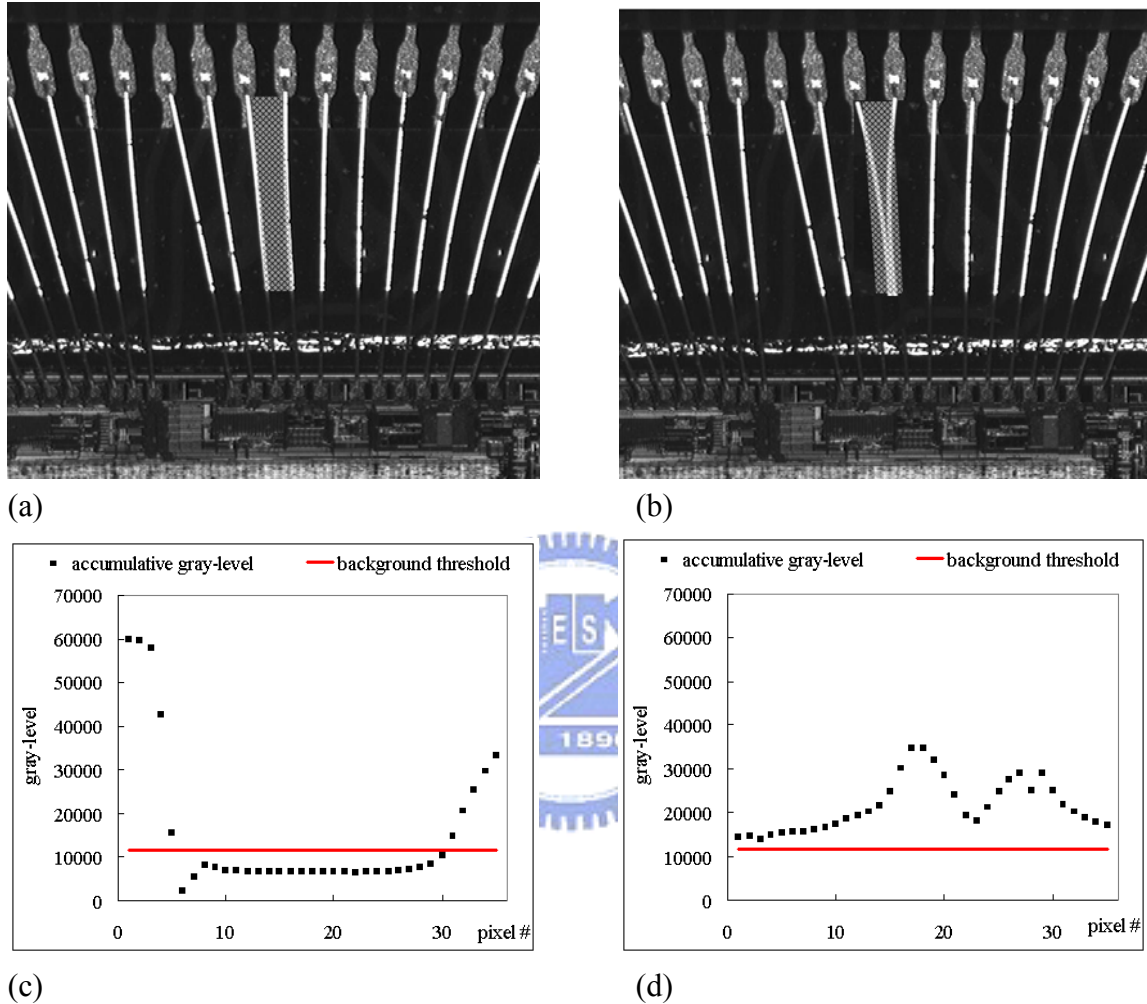
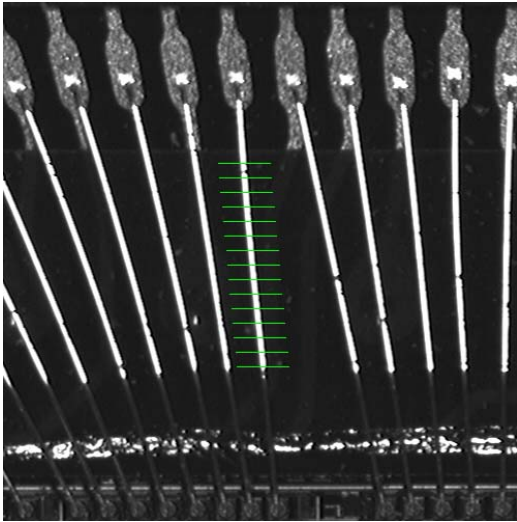


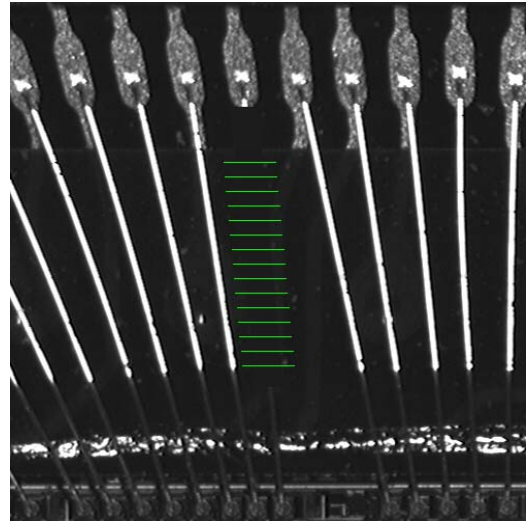
Figure 34. Experimentation of shorted wire inspection: (a) The grabbed image of the bonding wires in the north side of IC chip without shorted defect (b) the image with a man-made shorted defect. The meshed rectangular regions indicate the projection regions and the chart in (c) and (d), respectively, illustrates the projection result of Figures 34(a) and 34(b). The squares indicate the accumulative gray-level of the projection region and the horizontal lines indicate the threshold value of the background.

#### 6-4 Experimental result of lost wire inspection

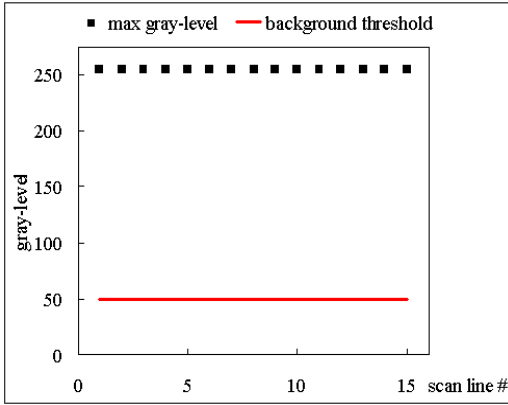
Figure 35(a) shows an image with normal bonding wires while Figure 35(b) shows an image with a man-made wire lost defect in the 6-th wire from the right. The horizontal lines in the two images indicate the scan lines for lost/broken/sagged wire defect inspection. Once a bonding wire disappeared on the scan line, the gray-level of each of the pixels of the bonding wire should be lower than the threshold value (say  $\mu+6\sigma$  of the gray-level of background). To save the inspection time, we only record each of the maximum gray-level of the pixels on each scan line. If each of the maximum gray-level of the scan lines is lower than the threshold value, then the inspected wire will be marked as a lost wire. The maximum gray-levels of the wires on the scan lines are shown in Figures 35(c) and 35(d). The squares indicate the maximum gray-levels of the wire on the scan lines and the horizontal lines indicate the threshold value of the background. Figure 35(c) corresponds to Figure 35(a) in which every maximum gray-level is 255. Figure 35(d) corresponds to Figure 35(b) in which every maximum gray-level is lower than the threshold value of the background. That is, the 6-th wire from the right in Figure 35(a) is a normal wire; while the 6-th wire from the right in Figure 35(b) is a lost one.



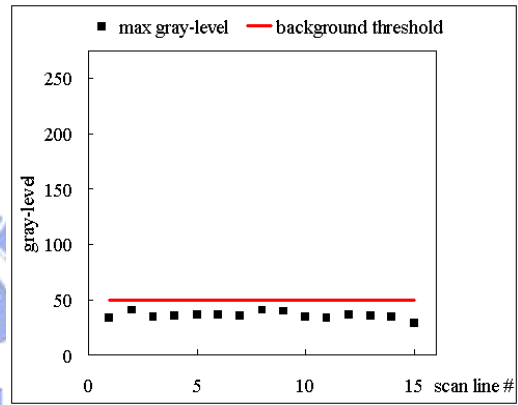
(a)



(b)



(c)



(d)

Figure 35. Experimentation of lost wire inspection: (a) The grabbed image of the normal bonding wires in the north side of IC chip and (b) the image with a man-made lost defect in the 6-th bonding wire from the right. The horizontal lines indicate the scan lines for lost/broken/sagged wire defect inspection. The (c) and (d), respectively, illustrates the maximum gray-levels of the wires on the scan lines in Figure 35(a) and 35(b). The squares indicate the maximum gray-levels of scan lines and the horizontal lines indicate the threshold value of the background

## 6-5 Experimental result of broken wire inspection

Figure 36(a) shows an image with a man-made broken defect in the 5-th wire from the right. The horizontal lines in the image indicate the scan lines for lost/broken/sagged wire defect inspection. If some of the maximum gray-levels of the scan lines are lower than the threshold value, then the inspected wire will be marked as a broken wire. The maximum gray-levels of the wire on the scan lines are shown in Figure 36(b). The squares indicate the maximum gray-levels of the wire on the scan lines and the horizontal line indicates the threshold value of the background. In Figure 36(b), some of the maximum gray-levels are lower than the threshold value of the background. That is, the 5-th bonding wire from the right in Figure 36(a) is a broken wire.

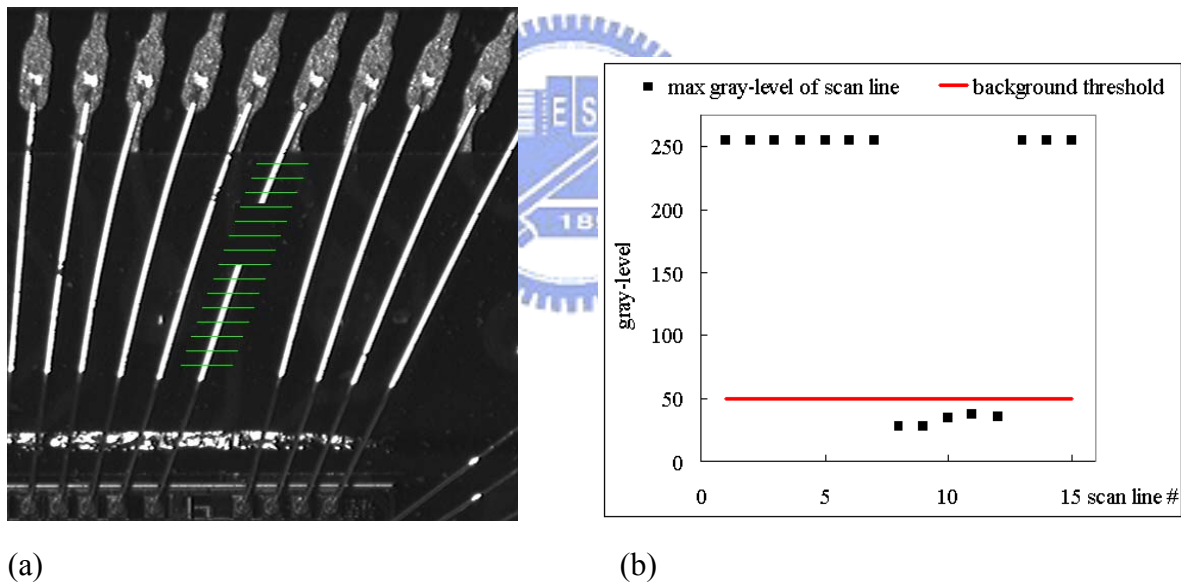


Figure 36. Experimentation of broken wire inspection: (a) The grabbed image of a broken defect in the 5-th bonding wire from the left and the corresponding scan lines for lost/broken/sagged wire defect inspection. (b) the maximum gray-levels of the wire on the scan lines in Figure 36(a), the squares indicate the maximum gray-levels of scan lines and the horizontal line indicates the threshold value of the background

## 6-6 Experimental result of sagged Wire Inspection

Figure 37(a) shows a grabbed image with two sagged wires and we take the most left one as the example to illustrate the experimentation. The horizontal lines in the image indicate the scan lines for lost/broken/sagged wire defect inspection. If each of the maximum gray-levels of scan lines is higher than the threshold value and some of the maximum gray-levels are lower than 255, the inspected wire will be marked as a sagged wire. The maximum gray-levels of the wire on the scan lines are illustrated in Figure 37(b). The squares indicate the maximum gray-levels of the wire on the scan lines and the horizontal line indicates the threshold value of the background. In Figure 37(b), the first four maximum gray-levels are lower than 255 but higher than the threshold value of the background. That is, the most left bonding wire in Figure 37(a) is a sagged wire.

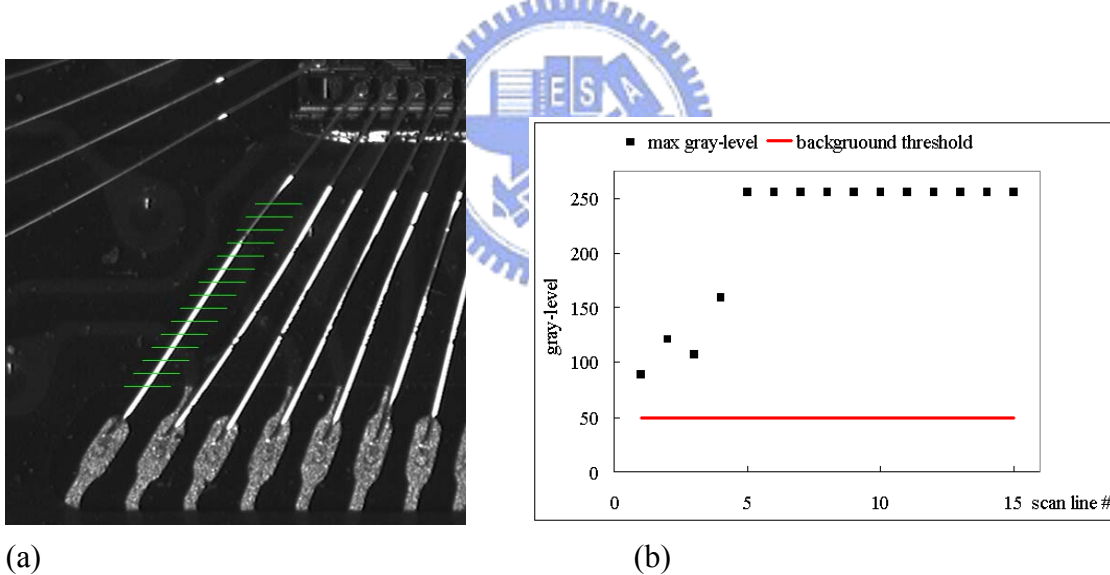


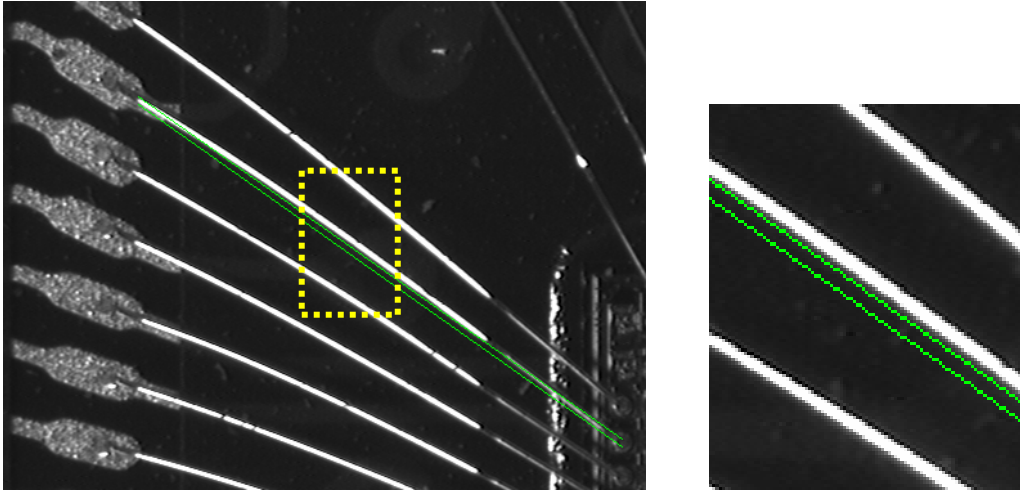
Figure 37. Experimentation of sagged wire inspection: (a) The grabbed image of a sagged defect in the most left bonding wire and the corresponding scan lines for lost/broken/sagged wire defect inspection. (b) the maximum gray-levels of the wire on the scan lines in Figure 37(a), the squares indicate the maximum gray-levels of scan lines and the horizontal line indicates the threshold value of the background

## 6-7 Experimental result of shifted wire inspection

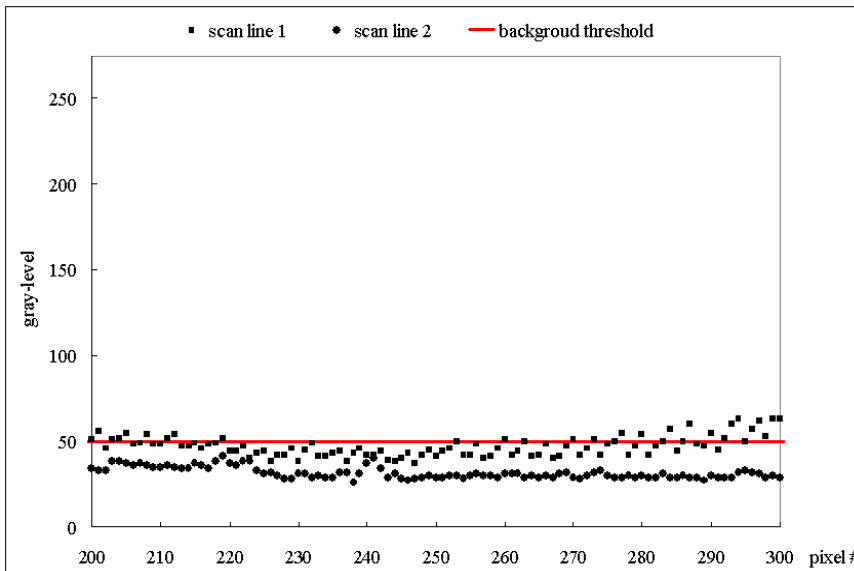
Figure 38(a) shows a grabbed image with a wire shifted defect in the second wire from the top. The two parallel lines in the image indicate the associated two scan lines for shifted wire defect inspection while the shifted allowance is set as one diameter of the wire. The two scan lines are set in the specified position of the two boundaries of a bonding wire, as described in Section 5-4. Figure 38(b) illustrates the gray-levels of the pixels on the two scan lines, the squares indicate the gray-levels of the pixels on scan line 1, the dots indicate the gray-levels of the pixels on scan line 2 and the horizontal line indicates the threshold value of the background. The gray-levels of the pixels on the two scan lines are lower than the background threshold in the middle segment. That is, the inspected wire is a shifted wire and the shifted distance is greater than the allowance, which is the diameter of the wire.







(a)

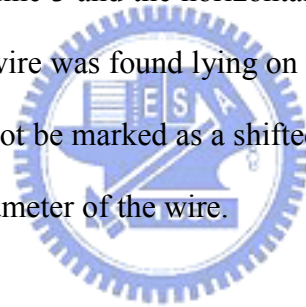


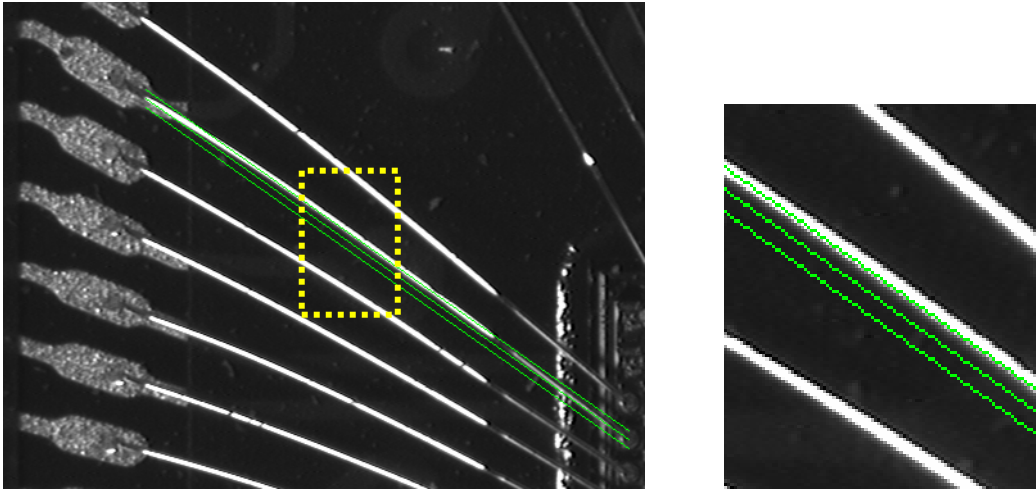
(b)

Figure 38. Experimentation of shifted wire inspection with the allowance in one diameter of the wire: (a) the image with a shifted bonding wire in the second from the top and the two parallel lines indicate the scan lines for shifted wire defect inspection. We enlarge the middle segment of the wire for clear representation. (b) The gray-level of the pixels on the two scan lines, the squares indicate the gray-levels of the pixels on scan line 1, the dots indicate the gray-levels of the pixels on scan line 2 and the horizontal line indicates the threshold value of the background

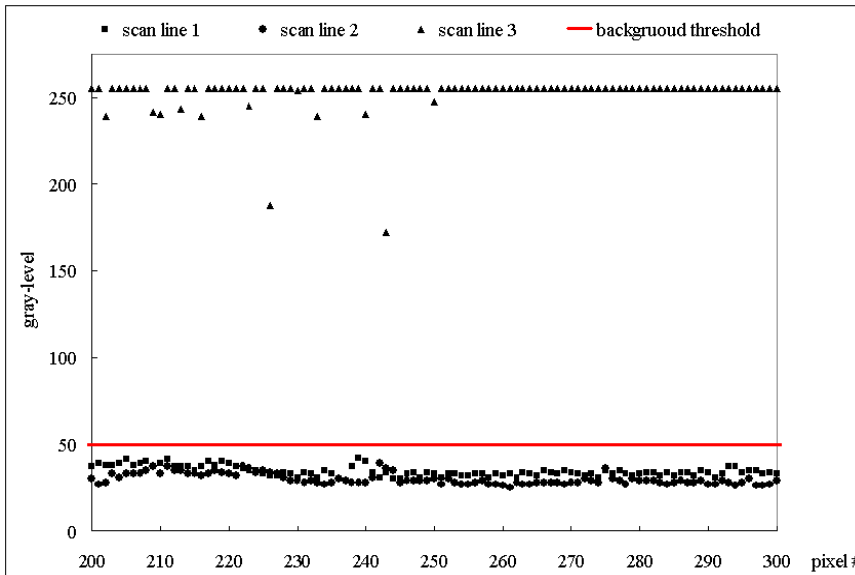


According to Section 5-4, we need to increase the number of scan lines for shifted wire inspection for larger allowable shifted distance. If the allowance of shifted distance is set as one and half times of the diameter of the bonding wire, the number of scan lines is set in three. The middle scan lines are set in the center of the specified position of the bonding wire. The distances between each two adjacent scan lines are also set as wide as the diameter of the bonding wire. Figure 39(a) shows a grabbed image with a shifted wire, which is the same one in Figure 38(a). The three parallel lines indicate the three scan lines for shifted wire inspection while the shifted allowance is set as one and half diameter of the wire. Figure 39(b) illustrates the gray-levels of the pixels on the three scan lines, the squares indicate the gray-levels of the pixels on scan line 1, the dots indicate that on scan line 2, the triangles indicate that on scan line 3 and the horizontal line indicates the threshold value of the background. The bonding wire was found lying on the scan line 3 in the middle segment, that is, this bonding wire will not be marked as a shifted wire with the larger shift allowance, which is one and half of the diameter of the wire.





(a)



(b)

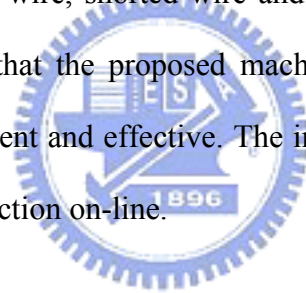
Figure 39. Experimentation of shifted wire inspection with the allowance in one and half diameter of the wire: (a) the same photo in Figure 38(a) and the three parallel lines indicate the three scan lines for shifted wire defect inspection. The middle segment of the wire is enlarged for clear representation. (b) the gray-level of the pixels on the three scan lines, the squares indicate the gray-levels of the pixels on scan line 1, the dots indicate the gray-levels of the pixel on scan line 2, the triangles indicate the gray-levels of the pixels on scan line 3 and the horizontal line indicates the threshold value of the background

## 7. Conclusions and Further Studies

### 7-1. Conclusions

In this dissertation, a machine vision system for the auto-inspection of wire bonding was first presented. A novel lighting environment, which can highlight the feature of the sagged bonding wire in the 2D image for 3D inspection purposes, was also first presented. By using the proposed lighting system, all the defects of bonding wire can be inspected in single 2D image.

A pattern matching method was developed to detect the position of the bonding ball. A set of inspection algorithms were developed to filter out all possible 2-D type error of broken wire, lost wire, shifted wire, shorted wire and the 3-D type error of sagged wires. Experimental results showed that the proposed machine vision system for wire bonding auto-inspection was very efficient and effective. The inspection speed of this system is fast enough for practical total inspection on-line.



### 7-2 Contributions

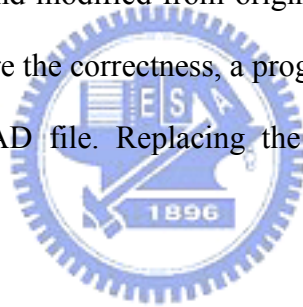
1. The reflection models of bonding ball and bonding wire are analyzed to search the proper lighting environment. A proper lighting device was proposed which can improve the quality of inspection image by omitting the background removing process. The reflection models can be applied to similar reflective objects, such as the weld points, on PCB.
2. A structured lighting system was proposed which enables a 2D image vision system to inspect the 3D defect of bonding wire. The inspection time for 3D wire defect can be greatly shortened to match with the bonding machine.
3. A set of efficient and effective algorithms for wire bonding are proposed. All the defects of bonding ball and wire can be inspected and classified accordingly in a very short

time.

### **7-3 Further Studies**

Few IC chips need special design, the multi-layer bonding wire, to connect more wires with the substrate. In the multi-layer IC chip, the bonding wires of various layers will cross in the top-view image and be inspected as shorted wires. By using the structured lighting system, the AOI system may grab the image of the bonding wires in single layer once and inspect the bonding wires successively. We will try to get the real sample of multi-layer IC chip to verify the effectiveness of the proposed structured lighting system.

The bonding program is the template in the inspection of bonding ball and wire. The bonding program is adjusted and modified from original CAD file by human operator and some error may occur. To ensure the correctness, a program is required to check the bonding program with the original CAD file. Replacing the human operator by an auto-adjust program is another solution.



## Reference

- [1] M. Ahmed, C. E. Cole, R. C. Jain and A. R. Rao, "INSPAD: A System for Automatic Bond Pad Inspection," IEEE Transactions on Semiconductor Manufacturing, vol.3, no.3, pp.145-147, 1990
- [2] A. Khotanzad, H. Banerjee and M. D. Srinath, "A Vision System for Inspection of Ball Bonds in Integrated Circuits," Proceedings of IEEE Workshop on Applications of Computer Vision, pp.290-297, 1992
- [3] A. Knotanzad, H. Banerjee and M. D. Srinath, "A Vision System for Inspection of Ball Bonds and 2-D Profile of Bonding Wires in Integrated Circuits," IEEE Transactions on Semiconductor Manufacturing, vol.7, pp.413-422, 1994
- [4] R. C. Gonzalez and R. E. Woods, Digital Image Processing, Addison-Wesley Publication, pp.419-420, 1987
- [5] N. Otsu, "Threshold Selection Method from Gray Level Histograms," IEEE Transactions on Systems, Man, and Cybernetics, SMC-9, pp.62-66, 1979
- [6] N. N. King and B. K. Sing, "Automated Inspection Of IC Bonding Wires Using Hough Transform," 14th Conference of Industrial Electronics Society, vol.4, pp.938-942, 1988
- [7] W. Zhang, L. M. Koh and Eddie M. C. Wong, "Computer Vision System for The Measurement of IC Wire-Bond Height," IEEE TENCON'93, pp.948-951, 1993
- [8] H. O. Lim, W. Zhang and L. M. Koh, "Automated Visual Inspection for IC Wire-Bond Using Auto-Focusing Technique," Fifteenth IEEE/CHMT International Electronic Manufacturing Technology Symposium, pp.31-36, 1993
- [9] Q. Z. Ye, S. H. Ong and X. Han, "A Stereo Vision System for The Inspection of IC Bonding Wires," International Journal of Imaging System Technology, vol.11, pp.254-262, 2000
- [10] M. Petuou, "Optimal Convolution Filters and an Algorithm for the Detection of Wide

- Linear Features,” IEEE Proceedings of Communications, Speech and Vision, vol.140, no.5, pp.331 – 339, 1993
- [11] R. M. Haralick and L. G. Shapiro, Computer and Robot Vision, Addison-Wesley, 1992
- [12] Y. F. Wang and D. I. Cheng, “3-D Shape Construction And Recognition By Fusing Intensity And Structured Lighting,” IEEE International Conference On Systems, Man, and Cybernetics, vol.2, pp.825-830, 1991
- [13] R. J. Woodham, “Photometric Method for Determining Surface Orientation From Multiple Images,” Optical Engineering, vol.19, no. 1, pp.139-144, 1980
- [14] A. C. Sanderson, L. E. Weiss and S. K. Nayar, “Structured Highlight Inspection of Specular Surfaces,” IEEE Transactions on Pattern Analysis and Machine Intelligence, vol.10, no.1, pp.44-55, 1988
- [15] T. L. Chia, Z. Chen and C. J. Yueh, “Curved Surface Reconstruction Using A Simple Structured Light Method,” IEEE Proceeding of the 13th International Conference on Pattern Recognition, pp.844-848, 1996
- [16] Y. L. Tian and H. T. Tsui, “3D Shape Recovery from Two-Color Image Sequences Using a Genetic Algorithm,” Proceedings of the 13th International Conference on Pattern Recognition, vol.4, pp.674-678, 1996
- [17] B. G. Batchelor, Automated Visual Inspection, Elsevier Science Publishing Company, pp.103-179, 1985
- [18] D. B. Perng, “Technique Report of Vision Laboratory,” Department of Industrial Engineering and Management, National Chiao-Tung University, Taiwan, 2004